Journal of Materials Chemistry B

Accepted Manuscript

ROYAL SOCIETY OF CHEMISTRY

www.rsc.org/materialsB

Journal of
Materials Chemistry B

RSCPublishing

ARTICLE

Amorphous carbon dots with high two-photon fluorescence for cellular imaging passivated by hyperbranched poly(amino amine)

Cite this: DOI: 10.1039/x0xx00000x

Received 00th January 2012,
Accepted 00th January 2012

DOI: 10.1039/x0xx00000x

www.rsc.org/

Gangsheng Tong,[*,†,a] Jingxia Wang,[†,b] Ruibin Wang,[a] Xinqiu Guo,[a] Lin He,[a] Feng Qiu,[c] Ge Wang,[a] Bangshang Zhu,[a] Xinyuan Zhu,[c] and Tao Liu[*,b]

Amorphous carbon dots (C-Dots) with high two-photon fluorescence were prepared by using citric acid (CA) as the carbon source and hyperbranched poly(amino amine) (HPAA) as the surface passivation agent through a facile hydrothermal approach. The C-Dots with an average diameter about 10 nm were readily dispersed in water. They exhibited excellent fluorescence properties and excitation-dependent fluorescence behavior with the corresponding quantum yield (QY) of 17.1 % in aqueous solution. Interestingly, the C-Dots emitted bright fluorescence with the QY of 16.3% even in a solid state which was the highest value for carbon-based nanomaterials. The C-Dots showed low cytotoxicity against L929 normal cells by using MTT assay. Furthermore, it could be easily internalized by HeLa cells and presented high quality one- and two-photon cellular imaging, suggesting the high potential application in biological imaging.

Introduction

Carbon dots (C-Dots) or carbon quantum dots generally refer to a class of small carbon nanoparticles with size around 10 nm, serendipitously discovered during the electrophoretic purification of single-walled carbon nanotubes (SWCNTs) in 2004.[1] Since then, due to the promising applications in the fields of bioimaging, medical diagnosis, catalysis and photovoltaic devices, many top-down or bottom-up approaches have been developed to obtain high quality C-Dots by adjusting the preparation method, varying the carbon source, modifying the post process, etc.[2-14] Through these unremitting efforts, the quantum yield (QY) was comparable with those of semiconductor quantum dots and organic dyes while they kept the unique properties such as non-photobleaching, non-blinking, good water solubility and biocompatibility. As the research moves along, two-photon fluorescence property has attracted much attention in the field of bioimaging due to its deep tissue penetration depth excited by near infrared light.[14-17] However, C-dots with two-photon fluorescence were usually synthesized via the "top-down" routes in strict conditions or required further surface modification for bioimaging.[14-16] Recently, the hydrothermal treatment was applied to prepare C-Dots with two-photon fluorescence but the QY was low.[17]

To improve the fluorescence properties, polymers or small molecules with amino groups had been widely used as the surface passivation agents for C-Dots.[17-19] However, without the polymer matrix or surface modification, the QYs were decrease greatly when they were aggregated or dried.[19-25] Therefore, if the passivation agent is not a fluorescence quenching polymer, the resulting C-Dots may have much different fluorescence properties. According to our latest research, hyperbranched poly(amino amine) (HPAA) was proved to be such a kind of polymer which emitted bright fluorescence light in a solid state.[26] Inspired by the above mentioned studies, we put forward one simple hydrothermal approach to prepare the one- and two-photon fluorescence C-Dots from HPAA and citric acid (CA) without further modification. The obtained C-Dots exhibited excellent fluorescence properties and excitation-dependent fluorescence behavior. The one- and two-photon cellular imaging results suggested their high potential in biological applications.

Experimental

Materials

Citric acid (CA, 99.9%) and *N*,*N*'-methylene bisacrylamide (MBA, 96%) were supplied by Sinopharm Chemical Reagent Co, Ltd. 1-(2-Aminoethyl) piperazine (AP, 99%), quinine sulfate (>98.0%) and 3-(4,5-dimethyl-thiazol-2-yl)-2,5-diphenyl tetrazolium bromide (MTT) were purchased from Sigma-Aldrich. All other chemicals were analytical-reagent grade and were used as received without any further purification. Ultrapure water was used in all experiments.

Characterization

The morphology and size of C-Dots were characterized by a transmission electron microscope (Tecnai G2 spirit Biotwin, FEI, USA). Size distribution and zeta potential were determined by a particle size and zeta potential analyzer (ZS90, Malvern,

UK). The crystallinity of C-Dots was confirmed using X-ray diffraction (XRD) (D8 Advance, Bruker, Germany). Raman spectra were measured with a Thermo Scientific DXR Raman Microscope (USA) with radiation at 780 nm. Fourier transform infrared (FTIR) spectra were recorded by a FTIR spectrometer (Paragon 1000, Perkin Elmer, USA). Thermogravimetric analysis (TGA) curves were obtained on a Perkin-Elmer TGA-7 instrument (USA) with a heating rate of 20 ^{o}C min^{-1} under nitrogen and air atmosphere, respectively. X-ray photoelectron spectroscopy (XPS) measurements were analyzed utilizing a Kratos AXIS Ultra X-ray photoelectron spectrometer (Shimadzu-Kratos, Japan) with Al Kα radiation (hν = 1486.6 eV), and the binding energies were calibrated by C 1s peak at 284.8 eV. UV-Vis absorption was conducted on a UV-Vis spectrometer (Lambda 20, Perkin Elmer, USA). Photoluminescence (PL) emission of C-Dots in aqueous solution and in a solid state was examined using a steady-state & time-resolved fluorescence spectrofluorometer (QM/TM/IM, PTI, USA). Two-photon spectra were performed on the SpectroPro300i (Roper Scientific, USA), its pump laser beam was from a modelocked Ti:sapphire laser system. The pulse duration was 200 fs, and the repetition rate was 76 MHz (Coherent Mira900-D).

Synthesis of HPAA

The cationic PAA with highly branched structure was synthesized by one-step reaction under a nitrogen atmosphere following the same procedure as our previous report.[26] The feeding mole ratio of *N*,*N*'-methylene bisacrylamide (MBA) and 1-(2-aminoethyl) piperazine (AP) was 1:1. Briefly, 3.15 g (20 mmol) MBA was dissolved in 30 mL water, then 2.61 g (20 mmol) of AP was added to the MBA solution under vigorous stirring. The polymerization was conducted at 60 °C under vigorous stirring for 60 h. After being concentrated, the solution was precipitated by acetone. Then it was dialyzed against ultrapure water for 2 days, and the clear, light yellow aqueous solution was obtained. Finally, the light yellow sticky solid was prepared under vacuum at 60 °C for 24 h. The physicochemical properties of HPAA were confirmed by GPC, FTIR and NMR. The molecule weight was determined as 8.0 × 10^3 Da with a branched degree of 0.44.[26]

Preparation of C-Dots

0.150 g HPAA was dissolved in 10 mL ultrapure water to form a homogeneous solution, followed by adding 1.051 g CA into the solution. The mixture was transferred into a 50 mL Teflon-lined stainless steel autoclave and kept at 200 ^{o}C for 3 h with a heating rate of 10 ^{o}C min^{-1}, then cooled to room temperature naturally. The color of the solution changed from light yellow to dark-brown. Subsequently, the aqueous solution was dialyzed against water using a dialysis membrane (MW cut-off = 1.0 × 10^4 Da) for 24 h.

Quantum yield

The QY of C-Dots in solution followed the equation below:

$$\frac{\phi}{\phi_R} = \frac{I}{I_R} \times \frac{A_R}{A} \times \frac{\eta^2}{\eta_R^2}$$

The calculation of QY was estimated by comparing the integrated PL intensity (excited at 360 nm) of the C-Dots with that of the quinine sulfate in 0.1 M H_2SO_4 (Φ_R = 54%).[17] Where, Φ refers to quantum yield and I is integrated emission intensity, A is the UV absorbance at the excitation wavelength. η is the refractive index of solvent. The subscript R refers to the reference fluorophore whose quantum yield has been well known. To minimize re-absorption effects, the absorbance in the 10 mm quartz cuvette was kept below 0.10 at the excitation wavelength.

While the QY of C-Dots in a solid-state was measured using an integrating sphere. Here, the calculation of QY_s was given by:

$$QY_s = \frac{N_{emission}}{N_{absorption}} = \frac{\alpha \int \frac{\lambda}{hc} \left[I_{em}(\lambda) - I'_{em}(\lambda) \right] d\lambda}{\alpha \int \frac{\lambda}{hc} \left[I_{ex}(\lambda) - I'_{ex}(\lambda) \right] d\lambda} = \frac{A_{em} - A'_{em}}{A_{ex} - A'_{ex}}$$

Where $N_{emission}$ and $N_{absorption}$ is the emitted and absorbed photon number of sample, respectively, α is the calibration factor of the measurement setup, h is plank's constant, c is the speed of light, $I_{em}(\lambda)$ is the PL intensity with sample, $I'_{em}(\lambda)$ is the baseline without sample, $I_{ex}(\lambda)$ is the intensity of the excitation light with sample, $I'_{ex}(\lambda)$ is the intensity of the excitation light without sample. A_{em} is the integral area of the emission curve line with sample, A'_{em} means the integral area of the emission curve line without sample, A_{ex} is the integral area of the excitation light with sample, A'_{ex} means the integral area of the excitation light without sample.[27]

Cell viability assay

The relative cytotoxicity of the C-Dots *in vitro* was assessed using MTT assay against mouse fibroblast L929 cells. Firstly, L929 cells were seeded into 96-well culture plates at a density of approximately 8 × 10^3 cells per well and incubated for 12 h at 37 ^{o}C under 5% CO_2. C-Dots with different concentrations (10, 20, 50, 100, 200 and 400 μg mL^{-1}) were added into each line. The cells coexisting with C-Dots were further incubated for 48 h at 37 ^{o}C under 5% CO_2. Subsequently, the medium was replaced with 200 μL fresh medium containing 20 μL of MTT (5 mg mL^{-1}). After incubation for another 4 h, all of the medium was removed and 150 mL DMSO was added to each well, followed by shaking for 15 min. The optical density of each well was immediately measured by BioTek® Synergy H4 at a wavelength of 490 nm. The cell viability was assessed and cells without any treatment in DMSO were used as control.

Cellular imaging

Human cervical carcinoma HeLa cells were seeded into a 6-well at 1.5 × 10^5 cells per well. The cells cultured for 18 h at 37 ^{o}C under 5% CO_2 in Dulbecco's modified Eagle medium (DMEM) mixed with 10% of fetal bovine serum (FBS). Then the HeLa cells were incubated with 100 μL C-Dots original solution mixed with 1.5 mL DMEM medium. After 2 h, the medium was removed, and the cells were washed with PBS 3 times. The cells were fixed by 4% paraformaldehyde in PBS, washed again with PBS and then observed with the inverted fluorescence microscope (DMI6000B) excited at 360 nm to get one-photon cellular imaging. Two-photon imaging was measured on a Nikon FN1 confocal microscopy (Japan) using 800 nm two-photon light.

Results and discussion

Synthesis and characterization of C-Dots

Carbohydrates are generally used as the carbon source to prepare C-Dots, though the specific mechanism is still hotly debated.[19,28] In this work, HPAA was used as the passivation agent to prepare C-

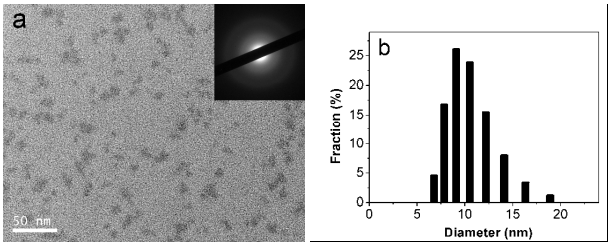

Fig. 1 TEM image (a) and DLS size distributions (b) for C-Dots. The inset scale bar is 50 nm.

Dots. Fig. 1 gives TEM image and DLS size distributions of the typical C-Dots. The statistical particle size distributions of C-Dots are mainly in the range of 7-17 nm with the peak at 10 nm. Furthermore, the diffuse ring in the SAED pattern reveals the amorphous nature of C-Dots. This result was further confirmed by XRD analysis (Fig. S1a). A broad peak appears at $2\theta = 19.15^{o}$ (0.46 nm), revealing the existence of amorphous carbon. However, due to the highly disordered carbon atoms and the strong PL interference excited under wavelengths ranging from the visible to the near infrared region, no obvious D or G bands were detected in the Raman spectra of C-Dots (Fig. S1b).[19, 29]

FTIR spectra were employed to identify the functional groups on the surface of C-Dots. As shown in Fig. 2, after the hydrothermal treatment, the O-H stretching of CA between 2500-3400 cm^{-1} becomes weak and the C=O stretching vibration of free carboxyl group at 1750 cm^{-1} disappears. As far as HPAA is concerned, the N-H stretching between 3100-3500 cm^{-1} significantly reduces, the N-H in-plane bending of the secondary amine at 1540 cm^{-1} and the C-N stretching of primary amine around 1110 cm^{-1} decrease drastically, accompanying by the enhancement of C=O stretching of amide group at 1654 cm^{-1} and N-H in-plane bending of tertiary amine at 1384 cm^{-1}. It confirms the amidation reaction between CA and HPAA. Besides, the double peaks of CA change into one peak at 1715 cm^{-1} of C-Dots which could be attributed to the formation of amide group or associated carboxyl groups. Furthermore, the detection of the C-O-C stretching at 1200 cm^{-1} verifies the incomplete dehydration reaction of CA. While the strong absorption around 2930 cm^{-1} refers to C-H antisymmetric and symmetric stretching which comes from the backbone of HPAA as well as the C-Dots. It is obvious that the C-Dots have many characteristic absorption bands of HPAA but less similar to those of CA. Thus, most of CA is carbonized while the HPAA fragments may be preserved during the hydrothermal treatment as the reports.[11, 29, 30]

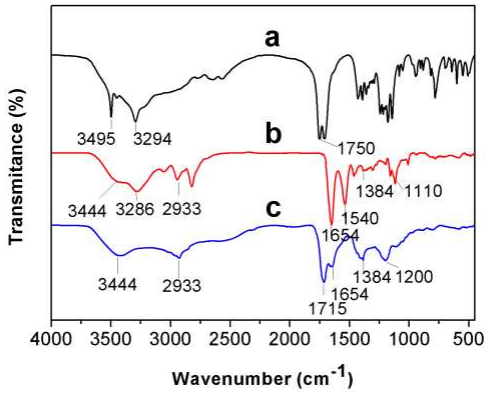

Fig. 2 FTIR spectra of (a) CA, (b) HPAA and (c) C-Dots.

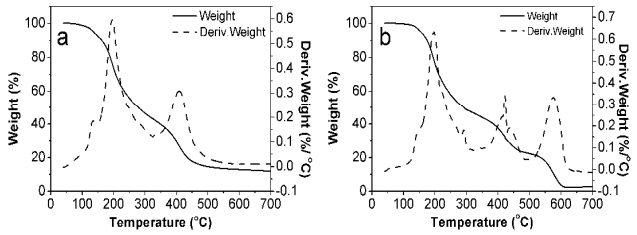

Fig. 3 TGA analysis of C-Dots under N_2 and air.

TGA analysis in Fig. 3 suggests that C-Dots are essentially stable at 110 °C and loss of weight afterwards. There is an obvious pyrolysis peak at 195 °C which is slightly above the decomposition temperature of CA. Therefore, this peak could be due to the degradation of the associated CA moieties with the C-Dots and the corresponding weight loss is about 50%. The peak at 420 ^{o}C is assigned to the pyrolysis of the HPAA fragments anchored strongly with the C-Dots via covalent linkages. The sample continues to oxidize at 576 ^{o}C in air, approximately 34 ^{o}C lower than graphene which is stable in air until 600 ^{o}C and at higher temperature,[7] then decomposed completely at 620 ^{o}C. By comparing the TGA curves under nitrogen and air atmosphere, the weight loss is about 16% that might be caused by the decomposition of carbon formed during the hydrothermal process. The TGA analysis further verifies that C-Dots are amorphous and composed of many CA moieties and HPPA fragments.

The surface functional groups of C-Dots were also determined by XPS. The survey spectrum of the C-Dots reveals three typical peaks of C 1S, N 1S and O 1S, as shown in Fig. 4a. It indicates that C, O and N appear on the surface of C-Dots, and the corresponding molar ratios are 64.2%, 34.0% and 1.8%, respectively. Moreover, the deconvolution of the C 1s spectrum in Fig. 4b reveals the presence of three types of carbon bonds: sp^2 C=C (284.8 eV), C-N (285.4 eV), C-O (286.2 eV) and C=O (289.0 eV).[11, 13] They represent the existence of carboxylic and hydroxyl groups, amide groups as well as the conjugated structures of C=C and C=O. The surface components of the C-Dots as determined by the XPS are in good agreement with FTIR and TGA results. In addition, the ξ potential of C-Dots is measured and the value is -30.7 mV similar with that of CA,[31] while that of the HPAA is +10.8 mV. It is clear that the surface of the C-Dots is covered with carboxyl groups. Therefore, the as-synthesized C-Dots are amorphous due to the introduction of oxygen-containing groups and polymer-like fragments.

Based on the experiments mentioned above, the plausible formation path of C-Dots is shown in Scheme 1. CA and HPAA firstly assemble by electrostatic interaction, then the two precursors condense to form hyperbranched polymer-like fragments.[11,19,32] Subsequently, CA is carbonized to generate lots of carbon cores (black sphere). Finally, with the core becoming larger and denser, the fragments are encapsulated in the nanoparticles or anchored on the surface and the cores are passivated simultaneously, resulting in the excellent fluorescent C-Dots.

The UV absorption and fluorescence properties are shown in Fig. 5. The UV spectrum of HPAA has two peaks, one is at 285 nm and the other is at 370 nm; while CA has no obvious absorption peak, as seen in Fig. 5a. After hydrothermal treatment, one peak of HPAA changes from 285 nm to 320 nm, which was ascribed to the n-π* transition of C=O bond in C-Dots;[11] the other peak is almost located at the same position with the second absorption peak of polymer. The brown solution shows bright blue fluorescence under the irradiation of 365 nm UV light lamp, as shown in Fig. 5a inset. As

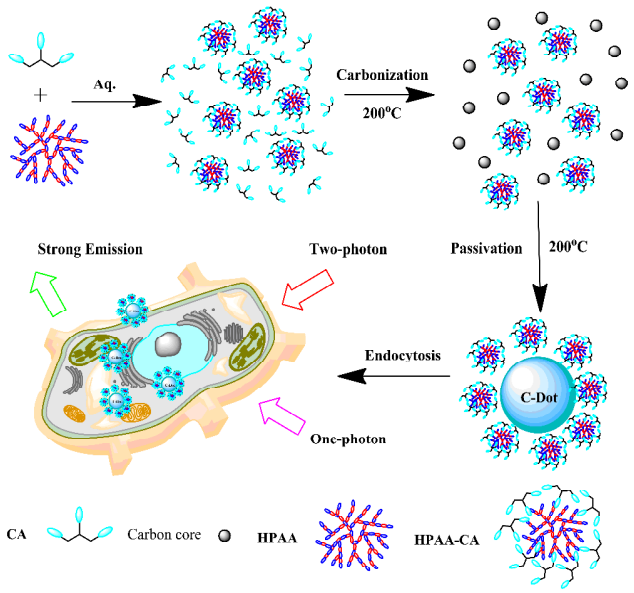

Scheme 1 Illustration of the formation of C-Dots from CA and HPAA via hydrothermal approach and the cellular imaging.

seen in Fig. 5b, with the increase of excitation wavelength from 300 to 420 nm, the emission wavelength of C-Dots shows red shift in aqueous solution gradually. The maximum emission wavelength is 450 nm under the excitation at 360 nm. This excitation-dependent PL behavior has also been identified as a generic feature of various types of C-Dots.[17,32] Using quinine sulfate as a reference chromophore, the QY of C-Dots of 17.1% is obtained under the excitation at 360 nm, as shown in Table S1. Furthermore, the average fluorescence lifetime of C-Dots was assessed by time-resolved photoluminescence measurements. Fig. 5c presents the fluorescence decay curve of C-Dots at 480 nm under the excitation at 405 nm. The average fluorescence lifetime is 11.02 ns, which is much longer than those of C-Dots reported before and many commercial fluorescent dyes.[33] In addition, there is no drastic reduction in PL intensity even after 5 h under continuous UV radiation (Fig. S2), confirming its good photo-stability. This high fluorescent intensity and the special excitation-dependent PL behavior of C-Dots could be used as potential tool for biological imaging.

To gain a better understanding of the observed photoluminescence, the C-Dots prepared following the same hydrothermal procedure from CA or HPAA were also synthesized, respectively. According to Fig. 5d, both of them have low PL intensity upon the excitation at 360 nm, while that of C-Dots

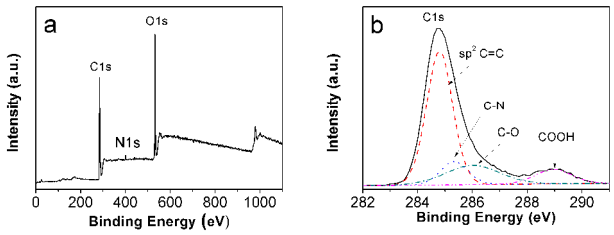

Fig. 4 a) A typical survey of XPS spectra of C-Dots b) C 1S high resolution XPS spectra of C-Dots with identification of peaks by curve fitting.

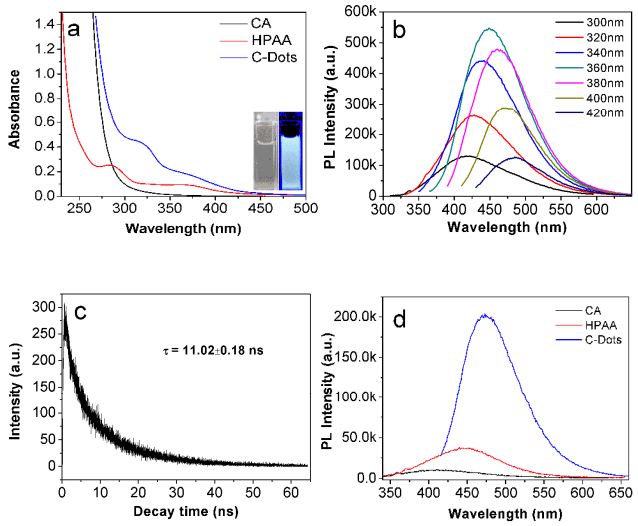

Fig. 5 (a) UV-Vis absorption spectra of CA, HPAA and C-Dots aqueous solution. Inset: digital photo taken with visual light (left) and UV light (right). (b) Excitation-dependent photoluminescence of C-Dots aqueous solution under the excitation wavelength of 300-420 nm with 20 nm of increment, (c) Fluorescence lifetime (ns) of C-Dots, (d) Comparison of photoluminescence intensity of C-Dots prepared from CA, HPAA, CA and HPAA. (All samples were hydrothermally treated following the same procedure).

obtained from CA and HPAA is almost 10 times stronger than the former two at the same concentration by area. It should be pointed out that CA contains no visible or near-UV chromophores, therefore no emission should be detected at visible wavelengths and the QY of the C-Dots prepared from CA by the same procedure is as low as 2.0%. The QY of HPAA in aqueous solution before and after the hydrothermal process is 1.5% and 4.7%, respectively. While the QY for the C-Dots reaches up to 17.1% in aqueous solution as shown in Table S1, about three times that of C-Dots prepared from HPAA. According to the results of XPS, FTIR and the ξ potential value, the as-synthesized C-Dots have different functional groups like COOH, C-O-C, C=O, and C-N on the surface which could result in a series of emissive traps between π and π^* states of C=C. When a certain excitation wavelength illuminates the C-Dots, a surface energy trap dominates the emission. As the excitation wavelength changes, another corresponding surface state emissive trap would become dominant which results in the excitation-dependent PL behavior.[11,34] Thus the high QY as well as the observed bright and colorful luminescence emission may be due to the surface-passivated process itself which forms the surface defects, molecular fluorophores and the carbon cores.[2,19,28]

After investigating the effect of the passivation polymer HPAA on the C-Dots' fluorescence properties, it was found that the PL intensity increases with the concentration and there was no obvious quenching even at high concentration (Fig. S3). What's more, C-Dots emit different bright fluorescence including blue, green, yellow and red at different excitation wavelength in a solid state as shown in Fig. 6. It might be very useful in multicolor imaging applications. The corresponding QY is much higher than that of HPAA in solid. In fact, the value is up to 16.3%, which is the highest in this field. It confirms that C-Dots have the similar fluorescence behavior as the passivation agent. The slight decrease of QY in solid state compared to the one observed in solution might be due to the different characterization methods and the quenching resulting from the incomplete passivation of C-Dots.

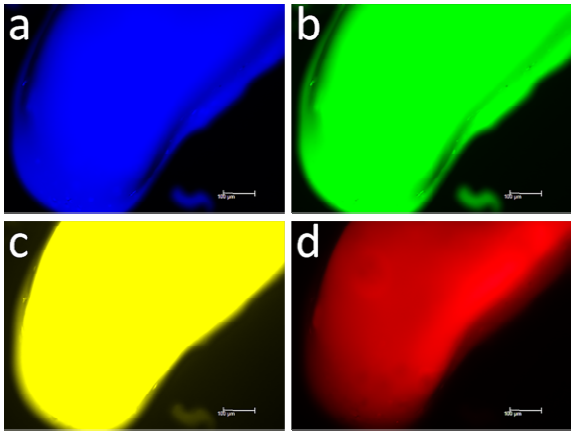

Fig. 6 Fluorescence images of C-Dots at different excitation wavelength. (a) 360 nm, (b) 450 nm, (c) 530 nm, (d) 580 nm.

Subsequently, the two-photon fluorescence property of C-Dots was measured. As shown in Fig. 7a, the PL intensity increases with the increment of the excitation laser power when the C-Dots are excited at 808 nm. Fig. 7b presents the obvious quadratic relationship between the fluorescence intensity and the excited laser power which indicates the good characteristic of two-photon fluorescence.[14,16] The two-photon absorption cross-section σ of C-Dots was measured by comparing the two-photon luminescence intensities of the sample with a reference under the same experimental conditions. By using rhodamine B as the reference, the average σ value for the C-Dots at 808 nm is estimated to be 16000 ± 1500 GM (Göeppert-Mayer unit, with 1 GM = 10^{-50} cm^4 s/photon). This value is half of the two-photon C-Dots prepared by "top-down" cutting routes which could attribute to the amorphous structure of C-Dots.[14-16] However, it is comparable to that of the semiconductor quantum dots and much higher than that of the organic dyes.[33] The high σ value for the C-Dots should be very beneficial for two-photon imaging and sensing in living cells and deep tissues.

Cytotoxicity evaluation of the C-Dots

In addition to the high photoluminescence intensity and good water solubility, the low cytotoxicity of C-Dots is the key properties for the practical biomedical applications. Therefore, the inherent cytotoxicity of C-Dots was evaluated using L929 cell line through MTT assay. As shown in Fig. 8, the whole evaluation shows dose-dependent cytotoxicity of C-Dots. It is notable that more than 80% of the cells are still viable even at a concentration of 400 μg mL^{-1}. It verifies that the biocompatibility of C-Dots is even better than the C-Dots prepared from PEG.[17]

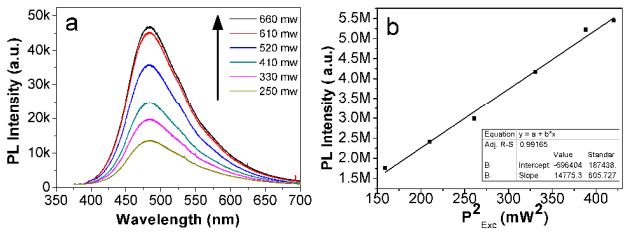

Fig. 7 (a) Two-photon photoluminescence (excitation wavelength = 808 nm) of C-Dots with different excitation power. (b) Fitting line based on the PL intensity and the corresponding excitation power.

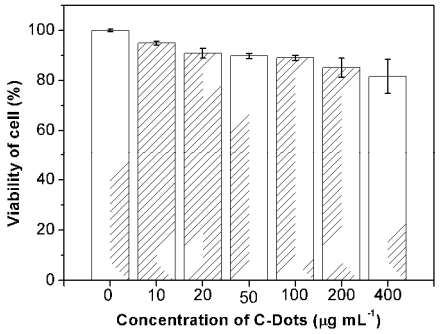

Fig. 8 Cell viability by MTT assay

Cellular imaging of C-Dots

Due to the remarkable luminescent characteristics with one- and two-photon light excitation, the as-synthesized C-Dots with low cytotoxicity were applied for cellular imaging. Fig. 9a and 9b display the bright field image and UV light excitation photographs of HeLa cells incubated with the C-Dots for 4 h, respectively. It is obvious that the C-Dots are internalized by HeLa cells which emit brilliant green light with the excitation of UV light at 365 nm.

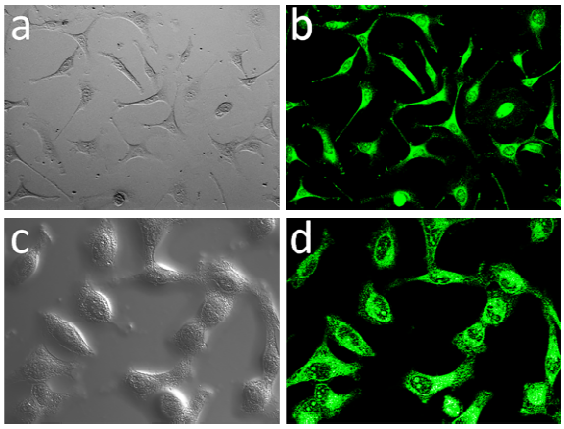

Fig. 9 One-photon cellular imaging under (a) bright field and (b) 365 nm (upper row), two-photon cellular imaging under (c) bright field and (d) 800 nm. (lower row).

Two-photon cell imaging has received much attention because of its many advantages such as low background signal, deep penetration depth and low phototoxicity with the help of near infrared excitation. As previously stated, the novel C-Dots naturally found the way to cellular imaging because of its two-photon fluorescence, good water solubility and biocompatibility etc. The cellular imaging was carried out to demonstrate the capability of the C-Dots for two-photon bioimaging. The two-photon bright field and fluorescence images (Fig. 9c, d) show that C-Dots are able to label the cell membrane, the cytoplasm and the nucleus of HeLa cells. However, it is different from the one-photon imaging that we can observed more detail information about the organelles from the two-photon imaging. The efficient cellular uptake, nontoxicity, and strong two-photon fluorescence show that the obtained C-Dots can be used as excellent two-photon probes for high contrast bioimaging.

Conclusions

In summary, we developed one simple hydrothermal approach to prepare the amorphous C-Dots with high two-photon fluorescence from HPAA and CA without further modification. The as-synthesized C-Dots exhibited excellent fluorescence properties and excitation-dependent fluorescence behavior with the corresponding QY of 17.1% in aqueous solution. Interestingly, the C-Dots emitted bright fluorescence with the QY of 16.3% even in a solid state which was the highest value for carbon-based nanomaterials. The MTT assay against L929 normal cells verified their low cytotoxicity. Furthermore, it could be easily internalized by HeLa cells and presented high quality one- and two-photon cellular imaging results, demonstrating the great potential applications for biomedical and bioimaging.

Acknowledgements

We are grateful for the financial support from the National Basic Research Program (2015CB931801), National Natural Science Foundation of China (21374062, 21376087, 51203089, 20104049, 51373099), the Open Project of State Key Laboratory of Chemical Engineering (SKL-ChE-12C04).

Notes and references

[a] Instrumental Analysis Center, Shanghai Jiao Tong University, 800 Dongchuan Road, Shanghai 200240, P. R. China. E-mail: tgs@sjtu.edu.cn

[b] UNILAB Research Center of Chemical Reaction Engineering, State Key Laboratory of Chemical Reaction Engineering, East China University of Science and Technology, 130 Meilong Road, Shanghai 200237, P. R. China, E-mail: liutao@ecust.edu.cn

[c] School of Chemistry and Chemical Engineering, State Key Laboratory of Metal Matrix Composites, Shanghai Jiao Tong University, 800 Dongchuan Road, Shanghai 200240, P. R. China.

† These authors contributed equally to this work.

‡ Electronic Supplementary Information (ESI) available: Fig. S1, Fig. S2, Fig. S3, Table S1. See DOI: 10.1039/b000000x/

1 X. Y. Xu, R. Ray, Y. L. Gu, H. J. Ploehn, L. Gearheart, K. Raker and W. A. Scrivens, *J. Am. Chem. Soc.*, 2004, 126, 12736.
2 Y. P. Sun, B. Zhou, Y. Lin, W. Wang, K. A. S. Fernando, P. Pathak, B. J. Meziani, B. A. Harruff, X. Wang, H. Wang, P. G. Luo, H. Yang, M. E. Kose, B. Chen, L. M. Veca and S. Y. Xie, *J. Am. Chem. Soc.*, 2006, 128, 7756.
3 H. Li, X. He, Z. Kang, H. Huang, Y. Liu, J. Liu, S. Lian, C. H. A. Tsang, X. Yang and S. T. Lee, *Angew. Chem. Int. Ed.*, 2010, 49, 4430.
4 P. G. Luo, S. Sahu, S. T. Yang, S. K. Sonkar, J. P. Wang, H. F. Wang, G. E. LeCroy, L. Cao and Y. P. Sun, *J. Mater. Chem. B*, 2013, 1, 2116.
5 W. Wang, Y. M. Li, L. Cheng, Z. Q. Cao and W. G. Liu, *J. Mater. Chem. B*, 2014, 2, 46.
6 X. Guo, C. F. Wang, Z. Y. Yu, L. Chen and S. Chen, *Chem. Commun*., 2012, 48, 2692.
7 A. Rahy, C. Zhou, J. Zheng, S. Y. Park, M. J. Kim, I. Jang, S. J. Cho and D. J. Yang, *Carbon*, 2012, 50, 1298.
8 S. Hu, R. Tian, L. Wu, Q. Zhao, J. Yang, J. Liu and S. Cao, *Chem. Asian J.*, 2013, 8, 1035.
9 H. P. Liu, T. Ye and C. D. Mao, *Angew. Chem. Int. Ed.*, 2007, 46, 6473.
10 H. Li, X. He, Y. Liu, H. Huang, S. Lian, S. T. Lee and Z. Kang, *Carbon*, 2011, 49, 605.
11 L. Tang, R. Ji, X. Cao, J. Lin, H. Jiang, X. Li, K. S. Teng, C. M. Luk, S. Zeng, J. Hao and S. P. Lau, *Acs. Nano.*, 2012, 6, 5102.
12 H. Zhu, X. Wang, Y. Li, Z. Wang, F. Yang and X. Yang, *Chem. Commun.*, 2009, 5118.
13 Q. Wang, X. Liu, L. Zhang and Y. Lv, *Analyst*, 2012, 137, 5392.
14 L. Cao, X. Wang, M. J. Meziani, F. Lu, H. Wang, P. G. Luo, Y. Lin, B. A. Harruff, L. M. Veca, D. Murray, S. Y. Xie and Y. P. Sun, *J. Am. Chem. Soc.*, 2007, 129, 11318.
15 B. Kong, A. Zhu, C. Ding, X. Zhao, B. Li and Y. Tian, *Adv. Mater.*, 2012, 24, 5844.
16 Q. Liu, B. Guo, Z. Rao, B. Zhang and J. R. Gong, *Nano Lett.*, 2013, 13, 2436.
17 R. J. Fan, Q. Sun, L. Zhang, Y. Zhang and A. H. Lu, *Carbon*, 2014, 71, 87.
18 B. F. Han, W. X. Wang, H. Y. Wu, F. Fang, N. Z. Wang, X. J. Zhang and S. K. Xu, *Colloid. Surface. B.*, 2012, 100, 209.
19 S. J. Zhu, Q. N. Meng, L. Wang, J. H. Zhang, Y. B. Song, H. Jin, K. Zhang, H. C. Sun, H. Y. Wang and B. Yang, *Angew. Chem.*, 2013, 125, 4045.
20 Z. Xie, F. Wang and C. Liu, *Adv. Mater.*, 2012, 24, 1716.
21 P. Zhang, W. Li, X. Zhai, C. Liu, L. Dai and W. Liu, *Chem. Commun.*, 2012, 48, 10431.
22 F. Wang, Y. Chen, C Liu and D. Ma, *Chem. Commun.*, 2011, 47, 3502.
23 F. Wang, Z. Xie, B. Zhang, Y. Liu, W. Yang and C. Liu, *Nanoscale*, 2014, 6, 3818.
24 Y. H. Deng, X. Chen, F. Wang, X. A. Zhang, D. X. Zhao and D. Z. Shen, *Nanoscale*, 2014, 6, 10388.
25 X. Zhang, Y. Zhang, Y. Wang, S. Kalytchuk, S. V. Kershaw, Y. Wang, P. Wang, T. Zhang, Y. Zhao, H. Zhang, T. Cui, Y. Wang, J. Zhao, W. W. Yu, and A. L. Rogach, *ACS nano*, 2013, 7, 11234.
26 R. B. Wang, L. Z. Zhou, Y. F. Zhou, G. L. Li, X. Y. Zhu, H. C. Gu, X. L. Jiang, H. Q. Li, J. L. Wu, L. He, X. Q. Guo, B. S. Zhu and D. Y. Yan, *Biomacromolecules*, 2010, 11, 489.
27 Y. Kawamura, H. Sasabe and C. Adachi, *Jpn. J. Appl. Phys.*, 2004, 43, 7729.
28 M. J. Krysmann, A. Kelarakis, P. Dallas and E. P. Giannelis, *J. Am. Chem. Soc.*, 2012, 134, 747.
29 C. Z. Zhu, J. F. Zhai and S. J. Dong, *Chem. Commun.*, 2012, 48, 9367.
30 H. F. Shurvell, Spectra-Structure Correlations in the Mid- and Far-infrared, Handbook of Vibrational Spectroscopy, *John Wiley & Sons Press*, 2006.
31 I. A. Mudunkotuwa and V. H. Grassian, *J. Am. Chem. Soc.*, 2010, 132, 14986.
32 Y. B. Song, S. J. Zhu and B. Yang, *RSC Adv.*, 2014, 2014, 4, 27184.
33 U. Resch-Genger, M. Grabolle, S. Cavaliere-Jaricot, R. Nitschke and T. Nann, *Nat. Methods*, 2008, 5, 763.
34 S. Sahu, B. Behera, T. K. Maiti and S. Mohapatra, *Chem. Commun.*, 2012, 48, 8835.

Amorphous carbon dots with high two-photon fluorescence for cellular imaging passivated by hyperbranched poly(amino amine)

Gangsheng Tong,* Jingxia Wang, Ruibin Wang, Xinqiu Guo, Lin He, Feng Qiu, Ge Wang, Bangshang Zhu, Xinyuan Zhu, and Tao Liu*

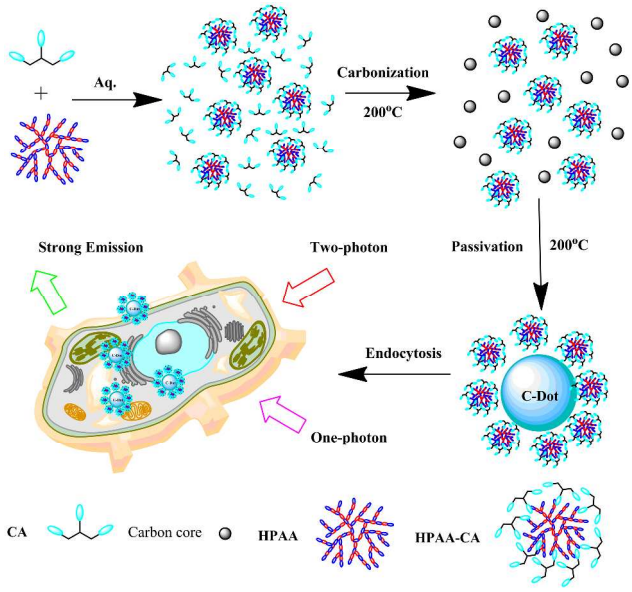

Amorphous carbon dots with high two-photon fluorescence in aqueous solution and solid state were prepared through a facile hydrothermal approach.